Food Chemistry: X 25 (2025) 102183

Contents lists available at ScienceDirect

Food Chemistry: X

journal homepage: www.sciencedirect.com/journal/food-chemistry-x

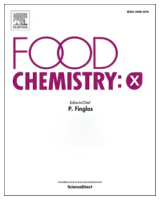

Effects of interactions between microorganisms and lipids on inferior volatile compound production during cold storage of grouper (*Epinephelus coioides*)

Yuanming Chu [a,c], Jinfeng Wang [a,b,e,*], Jing Xie [a,b,c,d,e,*]

[a] College of Food Science & Technology, Shanghai Ocean University, Shanghai, China
[b] Key Laboratory of Aquatic Products High Quality Utilization, Storage and Transportation (Co-construction by Ministry and Province), Ministry of Agriculture and Rural Affairs, Shanghai, China
[c] National Experimental Teaching Demonstration Center for Food Science and Engineering, Shanghai Ocean University, Shanghai, China
[d] Shanghai Engineering Research Center of Aquatic Product Processing & Preservation, Shanghai Ocean University, Shanghai, China
[e] Shanghai Professional Technology Service Platform on Cold Chain Equipment Performance and Energy Saving Evaluation, Shanghai Ocean University, Shanghai, China

ARTICLE INFO

Keywords:
Grouper
Lipids
Microorganism
Volatile compounds
Lipidomics
Cold storage

ABSTRACT

The interaction between microorganisms, proteins, and lipids plays a critical role in the odor production of fish. To explore the specific impact of the interaction between lipids and microorganisms on the overall odor of grouper, this study excluded the influence of proteins and assessed lipid (POV and TBARS) and microbial characteristics (biofilm mass and ATP content) in lipid solutions. The Results showed that microbial growth and lipid oxidation mutually promote each other. Lipidomics analysis identified 44 differential lipids, and microbial diversity analysis pinpointed five key microorganisms (*Carnobacterium*, *Pseudomonas*, *Gluconacetobacter*, *Vagococcus*, and *Shewanella*). Furthermore, 20 key volatile compounds (VOCs) related to odor changes in the grouper lipid solution were identified using HS-SPME-GC–MS. Correlation network analysis revealed potential microbial and lipid contributions to VOC categories, including alcohols, aldehydes, ketones, and nitrogen- and sulfur-containing compounds. This study provides new insights into the roles of microorganisms and lipids in flavor formation, offering valuable knowledge for improving seafood quality control.

1. Introduction

One of the most widely farmed marine fish in China is the grouper, highly valued by consumers for its nutritional benefits and rich taste (Chu et al., 2023a). With the increasing market demand and rising consumer expectations for taste, the quality of grouper has garnered significant attention. However, during storage, transportation, and retail, grouper experiences protein degradation and lipid oxidation due to endogenous enzyme reactions and microbial spoilage, leading to deterioration in product quality and safety (Yang et al., 2023). Consequently, there is growing interest in extending the shelf life of grouper to enhance its commercial value. Refrigeration at 4 °C is commonly used to prolong the shelf life of seafood and maintain its flavor (J. Wang et al., 2022). Despite this, microbial growth and metabolic activities that cause fish spoilage continue to occur under refrigerated conditions, alongside unavoidable protein and lipid degradation. These changes result in a decline in flavor quality, texture softening, and even spoilage of the seafood (Shui et al., 2022). Consequently, it is crucial to investigate the primary factors causing quality deterioration during refrigeration and explore methods to improve the quality of seafood.

Numerous studies have demonstrated that during aquaculture, transportation, processing, and storage, protein degradation, lipid oxidation, and microbial growth lead to flavor deterioration (Abd El-Hack et al., 2022; Y. Sun et al., 2022; Xue et al., 2022). However, it is well-known that seafood is a highly complex food matrix, with intricate interactions among microorganisms, lipids, and proteins, making it challenging to investigate the causes of quality deterioration (Zhuang et al., 2022). Therefore, it is necessary to separate these factors for individual study. Previous research has explored the mechanisms and pathways of producing undesirable VOCs when proteins and lipids act independently, and some potential solutions have been proposed (Chu et al., 2023a, 2023b). Nevertheless, the interactions among these factors

* Corresponding authors at: Shanghai Professional Technology Service Platform on Cold Chain Equipment Performance and Energy Saving Evaluation, Shanghai Ocean University, Shanghai, China.
E-mail addresses: jfwang@shou.edu.cn (J. Wang), jxie@shou.edu.cn (J. Xie).

https://doi.org/10.1016/j.fochx.2025.102183
Received 20 November 2024; Received in revised form 31 December 2024; Accepted 12 January 2025
Available online 13 January 2025

should not be overlooked.

Lipid oxidation plays a crucial role in generating undesirable VOCs, primarily contributing to the formation of aldehydes, ketones, and other carbonyl compounds (Liu et al., 2024). VOCs such as 2,4-heptadienal, 2,4-decadienal, and 2-hexenal are typical products of this process. Additionally, certain Gram-negative bacteria, including *Pseudomonas* and *Shewanella*, frequently act as spoilage microorganisms in seafood. These bacteria can reduce trimethylamine oxide to trimethylamine, causing off-flavors during the early stages of seafood spoilage (Yu et al., 2018). Theoretically, lipid oxidation and microbial growth influence each other in fish muscle. Oxidation products, such as hydroperoxides and carbonyl compounds, can be toxic to bacteria by potentially damaging DNA or interfering with cell signaling pathways (W. Deng et al., 1993). Furthermore, these oxidation products can alter the nutrient content and biochemical environment, thereby affecting microbial characteristics (Y. Deng et al., 2020). Additionally, certain bacteria in meat products produce lipases with lipid-degrading activity, releasing free unsaturated fatty acids and leading to more intense oxidation. Currently, there is a lack of comprehensive data on the interactions between microorganisms and lipid oxidation during the cold storage of seafood.

Lipidomics, as a powerful new strategy, can comprehensively describe lipid profiles, interactions among lipid molecules, and metabolic pathways. It can also identify lipid biomarkers by distinguishing different lipid types and elucidating their functional roles in organisms (Q. Li et al., 2017). Recent studies have focused on identifying biomarkers in seafood during storage (Fang et al., 2022; Tu et al., 2022; Yan et al., 2022). However, no research has yet explored the correlation between lipid oxidation and microbial characteristics during storage. Therefore, studying the interactions between lipids and microorganisms is novel.

In this study, factors related to protein oxidation were excluded, with a focus on the interactions between microorganisms and lipids and their mechanisms of influence on the production of undesirable VOCs. Relevant indicators for microorganisms and lipids were evaluated. Additionally, the generation of VOCs, particularly those that significantly impact the overall flavor of grouper, was monitored. During early, mid, and late storage periods, microbial community succession analysis was conducted alongside lipidomics analysis to investigate the molecular composition and structural characteristics of lipids in grouper during refrigeration. The study aims to identify distinctive lipid molecules and propose possible oxidation pathways. Furthermore, microbial community data are correlated with lipid molecular data to identify highly associated microorganisms and lipid molecules, determining the main contributors to characteristic flavor formation and potential formation pathways of grouper during cold storage. The findings will help elucidate the interactions between microorganisms and lipids during the cold storage of grouper, providing new insights for delaying spoilage and the production of undesirable VOCs during cold storage.

2. Material and methods

2.1. Preparation of experimental samples

2.1.1. Extraction of grouper lipid

To minimize inter-sample differences, a total of 20 live groupers were used in this study. These fish were purchased from an aquaculture supermarket that collaborates with the laboratory. With the assistance of staff, all the fish were euthanized by beating head, after which the head, viscera, and spine were removed (The slaughtering process of grouper complies with SHOU-DW-2023-087). The groupers were then placed in crushed ice and transported to the laboratory for lipid extraction.

Lipid extraction was conducted with slight modifications based on a previously described method (Chu et al., 2023b). Specifically, 100 g of grouper sample was extracted with 300 mL of chloroform-methanol solution (2,1, *v*/v), and the organic solvents were evaporated at 40 °C using a rotary evaporator. The resulting lipids were then mixed with methanol in a 1.5:1 ratio for further use.

2.1.2. Extraction of grouper bacteria and determination of research period

The bacteria used in this study were isolated from spoiled grouper. Initially, the grouper was prepared according to the method described in Section 2.1.1. These bacteria were revived using tryptic soy broth (TSB; Qingdao Hope Biotechnology Co., Ltd., Qingdao, China) for further experimentation. To accurately assess the interaction between microorganisms and lipids during growth, growth curves of grouper bacteria were determined. Initially, bacterial strains were activated by culturing in TSB for 12 h at 30 °C. Subsequently, 1 mL of logarithmic-phase bacterial solution was transferred to conical flasks containing 150 mL of TSB, and then incubated at 4 °C. The optical density (OD) was measured every 12 h, and growth curves were plotted, as shown in Fig. 1A. At 4 °C, the bacterial growth cycle lasted approximately 10 days. Therefore, considering the bacterial growth cycle, the experimental period was set to 10 days.

2.1.3. Preparation of sample solution

1 mL of activated logarithmic-phase grouper bacteria (M group) and lipid solution (L group) were separately added to conical flasks containing 150 mL of TSB as two control groups. Additionally, both were added together into conical flasks containing 150 mL of TSB as the experimental group (M/L group). It is worth noting that the lipid content in the L group and M/L group was 5 % (*v*/v). Subsequently, the three groups of samples were incubated on a shaker at 4 °C for 10 days. Microbial and lipid related characteristics were measured at 0, 2, 4, 6, 8, and 10 days. Microbial composition, lipid composition, and volatile compound content were determined at 6 and 10 days. The experimental procedure is illustrated in Fig. 1B.

2.2. Microbial related characteristics

2.2.1. Biofilm mass

Quantitative analysis of biofilm was performed using crystal violet staining method (P. Li et al., 2022). Briefly, bacterial suspension from different groups was transferred to a plate and incubated at 4 °C for 24 h. To remove non-adherent cells, the biofilms were gently washed three times with PBS (0.01 M, pH 7.0). Following fixation at 60 °C for 30 min, the biofilms were stained with 1 mL of crystal violet solution (0.2 %, *w*/*v*) for 15 min, after which excess dye was removed with PBS. Finally, 1 mL of ethanol (95 %, *v*/v) was added to dissolve the dye for 5 min, and absorbance was measured at 600 nm.

2.2.2. Quantification of ATP

Accurately transfer 0.1 mL of the thoroughly shaken sample solution and mix it with 1 mL of extraction solution in an ice bath. Add 500 μL of chloroform and shake vigorously to mix. Centrifuge the mixture at 10,000 *g* at 4 °C for 3 min, then carefully collect the supernatant and place it on ice for further analysis. Subsequently, follow the instructions of the ATP detection kit (Solarbio Technology Co., Ltd., Beijing, China) for detection.

2.3. Lipid related characteristics

2.3.1. Peroxide value (POV)

The determination of POV was conducted according to a Chinese National Standard (GB5009.227–2016) with slight modifications. 5 mL of the sample solution was mixed with 30 mL of a chloroform-ice acetic acid mixture (1:1.5, *v*/v) and shaken thoroughly. Then, 1.00 mL of saturated potassium iodide solution was added and shaken for 30 s. The mixture was allowed to stand in the dark for 3 min, after which 100 mL of ultrapure water was added and mixed well. The iodine released was then titrated with 0.002 mol/L sodium thiosulfate standard solution

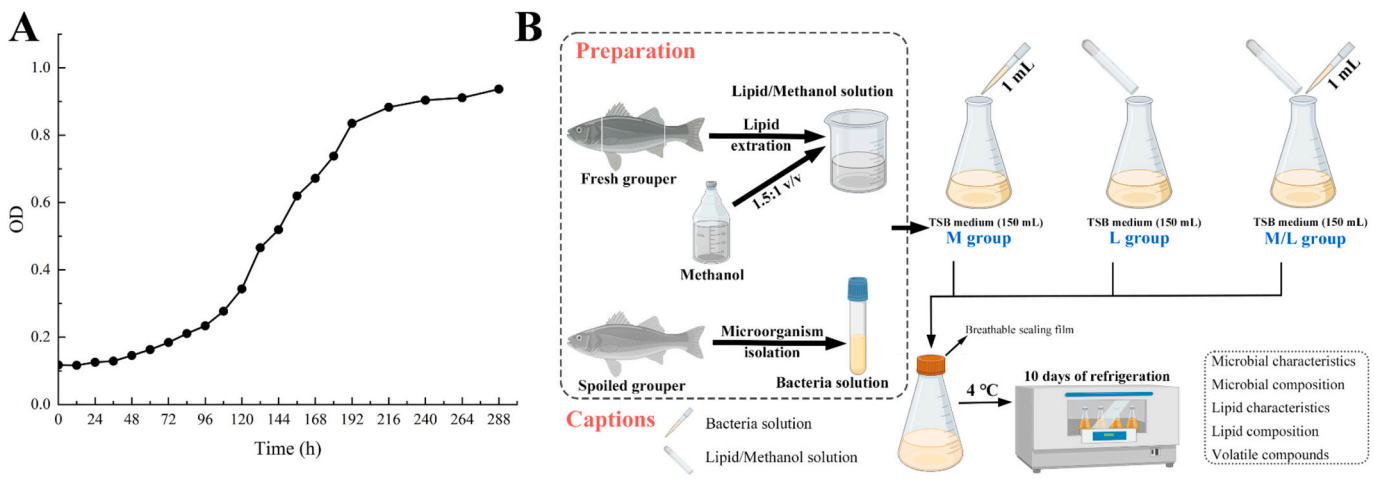

Fig. 1. The growth curve of bacteria (A), and schematic diagram of experimental design (B).

until the solution turns pale yellow. Finally, 1 mL of starch indicator was added, and the titration was continued until the blue color disappears. Record the volume of standard sodium thiosulfate solution consumed. Blank experiments were conducted simultaneously. The POV was calculated using the following formula:

$$POV = \frac{(V - V_0) \times c \times 0.1269}{v} \times 100$$

where, V and V_0 represent the volume of standard sodium thiosulfate solution consumed during the titration and in the blank experiment, respectively, in mL; c represents the concentration of the standard sodium thiosulfate solution, 0.002 mol/L; v represents the volume of the sample solution, 5 mL. The POV result is expressed as g/100 mL of sample solution.

2.3.2. Thiobarbituric acid reactive substances (TBARS)

The determination of TBARS followed a Chinese National Standard (GB 5009.181–2016) with some modifications. Accurately transfer 5 mL of the sample solution and mix it with 25 mL of trichloroacetic acid solution (TCA, 10 %, *v*/v), and vortex for 30 s. Subsequently, use ultrapure water to dilute the solution to 50 mL. Mix 5 mL of the resulting clear solution with 5 mL of 0.02 M thiobarbituric acid (TBA) and incubate in a water bath at 90 °C for 20 min. After natural cooling, measure the absorbance at 532 nm using a UV–visible spectrophotometer. Blank tests were conducted using distilled water instead of the sample solution. TBARS was calculated using the following formula and expressed as mg MDA/L of sample solution:

$$TBARS = A_{532} \times 7.8$$

where, A_{532} represents the absorbance at 532 nm; "7.8" is a constant.

2.4. VOCs

The VOCs were extracted from the sample solution using headspace solid-phase microextraction (HS-SPME). A 10 mL sample solution was added to the headspace vial, and the procedures and parameters were set according to Chu et al. (2024). The concentration of the target VOCs was calculated using the following equations:

$$C_X = A_X \times C_{IS}/A_{IS}$$

where C represents concentration (μg/L sample solution); A represents peak area.

2.5. Analysis of microbial community diversity and dynamics

The total DNA from the sample solution was extracted following the method described by Zhang et al. (2021), and the DNA concentration was quantified. The quality of the DNA extraction was assessed using 1.2 % agarose gel electrophoresis. The bacterial 16S rRNA V3-V4 region was amplified using primers 319F (5'-ACTCCTACGGGAGGCAGCAG-3′) and 806R (5'-GGACTACHVGGGTWTCTAAT-3′). The PCR amplification products were validated according to he protocol outlined by Deng et al. (2020). Subsequently, PCR products were sequenced using the Illumina MiSeq platform (Illumina, San Diego, California, USA) by Suzhou Panomix (Suzhou, China). Species annotation was performed for each Amplicon sequence variant (ASV) or Operational taxonomic unit (OTU) representative sequence using pre-trained Naive Bayes classifier in QIIME2 software.

2.6. Lipidomic

The lipid extraction from the sample solution was performed using a chloroform-methanol solution (2,1, *v*/v). Chromatographic separation was conducted using an ACQUITY UPLC® BEH C18 column (2.1 × 100 mm, 1.7 μm, Waters) maintained at 50 °C, with the autosampler temperature set at 8 °C. The analytes were eluted with a gradient of acetonitrile: water (60,40) containing 0.1 % formic acid and 10 mM ammonium formate (A2) and isopropanol: acetonitrile (90,10) with 0.1 % formic acid and 10 mM ammonium formate (B2), at a flow rate of 0.25 mL/min.

For ESI-MSn experiments, the spray voltage was set to 3.5 kV and 2.5 kV in positive and negative modes, respectively. Data dependent acquisition (DDA) MS/MS experiments were conducted with HCD scan, using a normalized collision energy of 30 eV. Dynamic exclusion was implemented to eliminate redundant information in MS/MS spectra.

2.7. Statistical analysis

All tests were conducted in triplicate, with results expressed as the mean ± standard deviation (SD). ANOVA was conducted on all experimental data using SPSS 26 (Chicago, US), followed by Duncan's test to determine significance. Visualization of the data was performed using Origin 2024b software (OriginLab Corp., Northampton, USA). Dimensionality reduction analysis of the lipid composition differences between samples was performed using orthogonal partial least squares discriminant analysis (OPLS-DA). Lipidomics data and Mantel test analyses were processed using the platform provided by Suzhou Panomix (https://www.biodeep.cn/).

3. Results and discussion

3.1. Lipid related characteristics

Lipid oxidation is widely recognized as a primary cause of quality degradation in fish products, significantly affecting their flavor, texture, color, and shelf life. Studies have shown that lipid oxidation and hydrolysis are inevitable, with lipid hydrolysis promoting oxidation during production and storage (Santos et al., 2019). During refrigeration, seafood lipids are highly susceptible to oxidation, leading to the formation of peroxides and other intermediate products. To evaluate the extent of lipid oxidation during storage, POV and TBARS values of the lipid sample solution were measured (Fig. A-B). POV indicates the level of primary oxidation products in lipids, assessing the initial stage of lipid oxidation in seafood (Zhou et al., 2019). Results showed that the initial POV of the lipid sample solution was 23.35 mg/100 mL. After 10 days of storage at 4 °C, the POV increased to 81.05 mg/100 mL. Samples with added grouper bacteria (M/L group) also exhibited a similar increasing trend, from 22.67 mg/100 mL to 93.74 mg/100 mL. However, from day 6 onwards, the POV in the treatment group was significantly higher than in the control group. These findings suggest that the addition of grouper bacteria promotes primary lipid oxidation during refrigeration.

Malondialdehyde (MDA) is a key oxidation product of polyunsaturated fatty acids, representing secondary lipid oxidation (X. Huang et al., 2023). The extent of secondary lipid oxidation can be assessed by measuring the quantity of MDA through its reaction with colorimetric substances (Silveira Alexandre et al., 2022). Generally, higher TBARS values indicate increased MDA formation and lipid oxidation levels. As shown in Fig. 2B, the TBARS values of the lipid sample solution during refrigeration initially measured 0.52 mg MDA/L for the L group and 0.49 mg MDA/L for the M/L group, gradually increasing to 2.26 mg MDA/L and 2.80 mg MDA/L, respectively. This indicates ongoing secondary oxidation of the lipids in the grouper. Notably, TBARS values in the M/L group were consistently higher than those in the L group during storage, with significant differences observed from day 6 onwards, reaching 0.53–1.01 mg MDA/L. A study by Aracati et al. (2022) found a correlation between increased psychrotrophic microorganisms and TBARS in tilapia fillets, suggesting that the grouper bacteria in the sample solution entered the logarithmic growth phase around day 6, leading to increased TBARS. This is consistent with the POV analysis results.

3.2. Microbial related characteristics

The formation of biofilms is a complex and dynamic process involving initial attachment, irreversible attachment, biofilm maturation, and biofilm dispersion (Mukherjee et al., 2020). To better understand the dynamic formation of grouper bacterial biofilms under the influence of lipid oxidation, the biofilm mass was measured, as shown in Fig. 2C. Both sample solutions exhibited a trend of initial increase

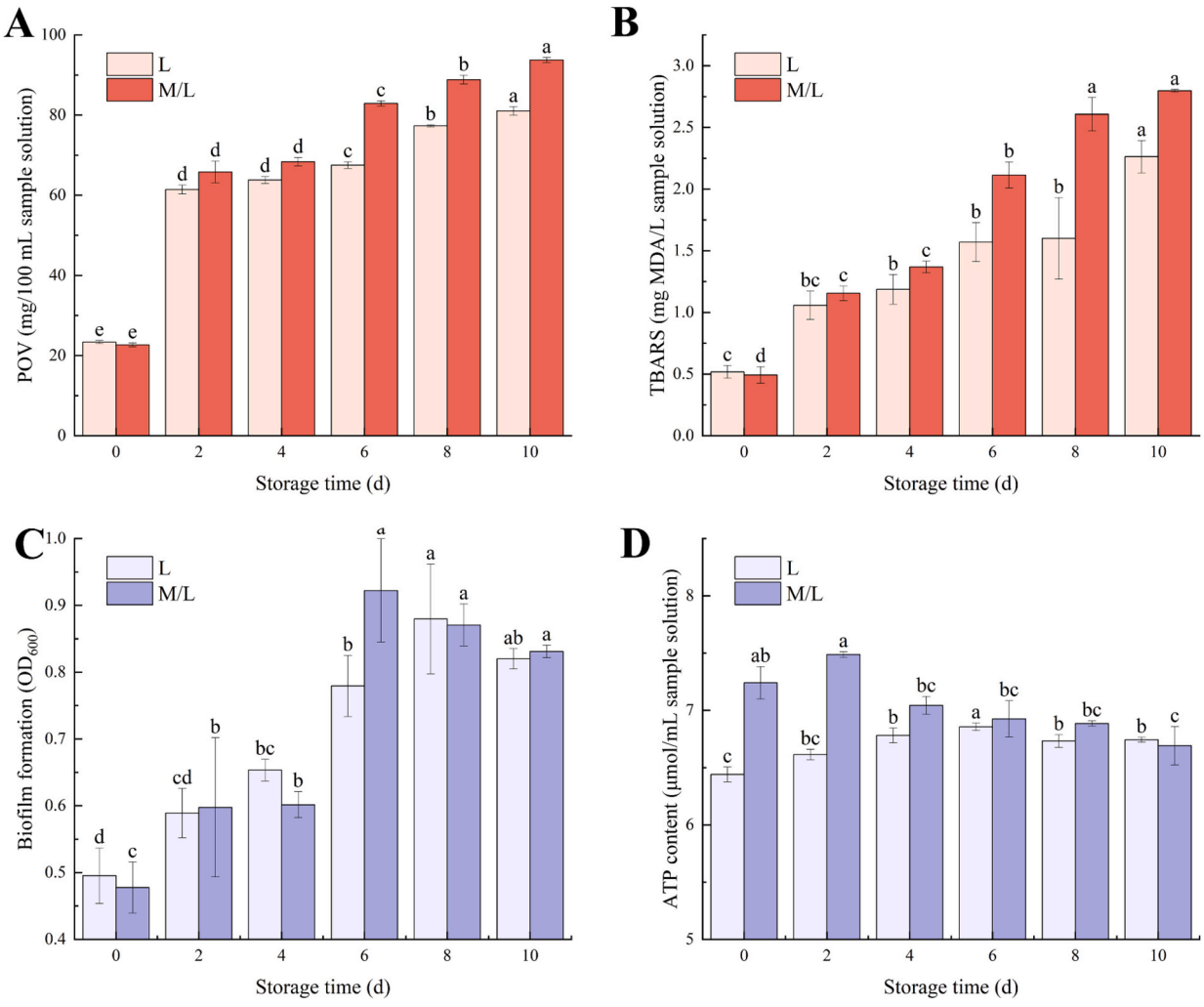

Fig. 2. POV (a), TBARs (b) of groupers; biofilm mass (c), and ATP content (d) of different sample solution. Mean values with different lowercase letters are significantly different at $p < 0.05$.

followed by a decrease, indicating a transition from biofilm maturation to dispersion. The biofilm formation in the M group progressed relatively slowly, peaking at an OD600 value of 0.880 on day 8. A study by Aiassa et al. (2014) demonstrated that free radicals can directly attack polyunsaturated fatty acids (PUFAs) in biological membranes. Free radicals such as HOO•, O_2•-, singlet oxygen, and ozone can initiate peroxidation of unsaturated fatty acids and trigger chain reactions (Soler-Arango et al., 2019). This primarily affects membrane fluidity, altering membrane characteristics and significantly disrupting membrane-bound proteins. This amplification effect can generate more free radicals, degrading PUFAs into various products. Consequently, after day 8, the biofilm mass in the M group gradually decreased due to lipid oxidation within the membrane. In contrast, the sample solution containing lipids (M/L group) reached the maturation stage by day 6, with an OD600 value of 0.922, indicating better biofilm growth compared to the M group. This might be because, while free radicals attack the lipids within the biofilm, they also target the added grouper lipids in the solution, thereby relatively reducing the attack on the bacterial biofilm. Overall, the lipid oxidation process in the grouper helped maintain the stability of the grouper bacterial biofilm and promoted microbial growth.

Adenosine triphosphate (ATP) is a fundamental carrier for energy conversion, playing a crucial role in nutrient processing, macromolecule synthesis, and enzyme secretion (Wu et al., 2022). The ATP content in the two groups of sample solutions during refrigeration was measured, as shown in Fig. 2D. The results exhibited a trend similar to the changes in biofilm mass. Throughout the storage period, the ATP content in the M/L group was significantly higher than that in the L group, indicating enhanced microbial metabolism in the M/L group, consistent with the findings on biofilm mass. Under cold stress conditions, disruption of cellular homeostasis and integrity can lead to changes in energy metabolism (Tian et al., 2021). The biofilm structure in the L group was more severely damaged compared to the M/L group, resulting in reduced metabolic capability and lower ATP content.

Based on the analysis and discussion in sections 3.1 and 3.2, it is evident that microbial growth and lipid oxidation interact with each other: microbial growth promotes lipid oxidation, and the oxidation of grouper lipids, in turn, enhances microbial growth. To gain a deeper understanding of the relationship between grouper lipid oxidation and microbial growth, further analysis of the lipid composition and microbial community in the sample solutions during refrigeration was conducted. This analysis aims to elucidate the mechanisms underlying the interaction between grouper lipids and microorganisms.

3.3. Lipidomics

3.3.1. Lipid composition analysis

Lipidomics analysis using LC-MS identified and classified the lipid species present in the lipid sample solutions (L group and M/L group). A total of 1467 lipids were identified, categorized into 37 lipid classes, including triacylglycerols (TGs, 534 species, 36.40 %), phosphatidylcholines (PCs, 245 species, 16.70 %), diacylglycerols (DGs, 145 species,

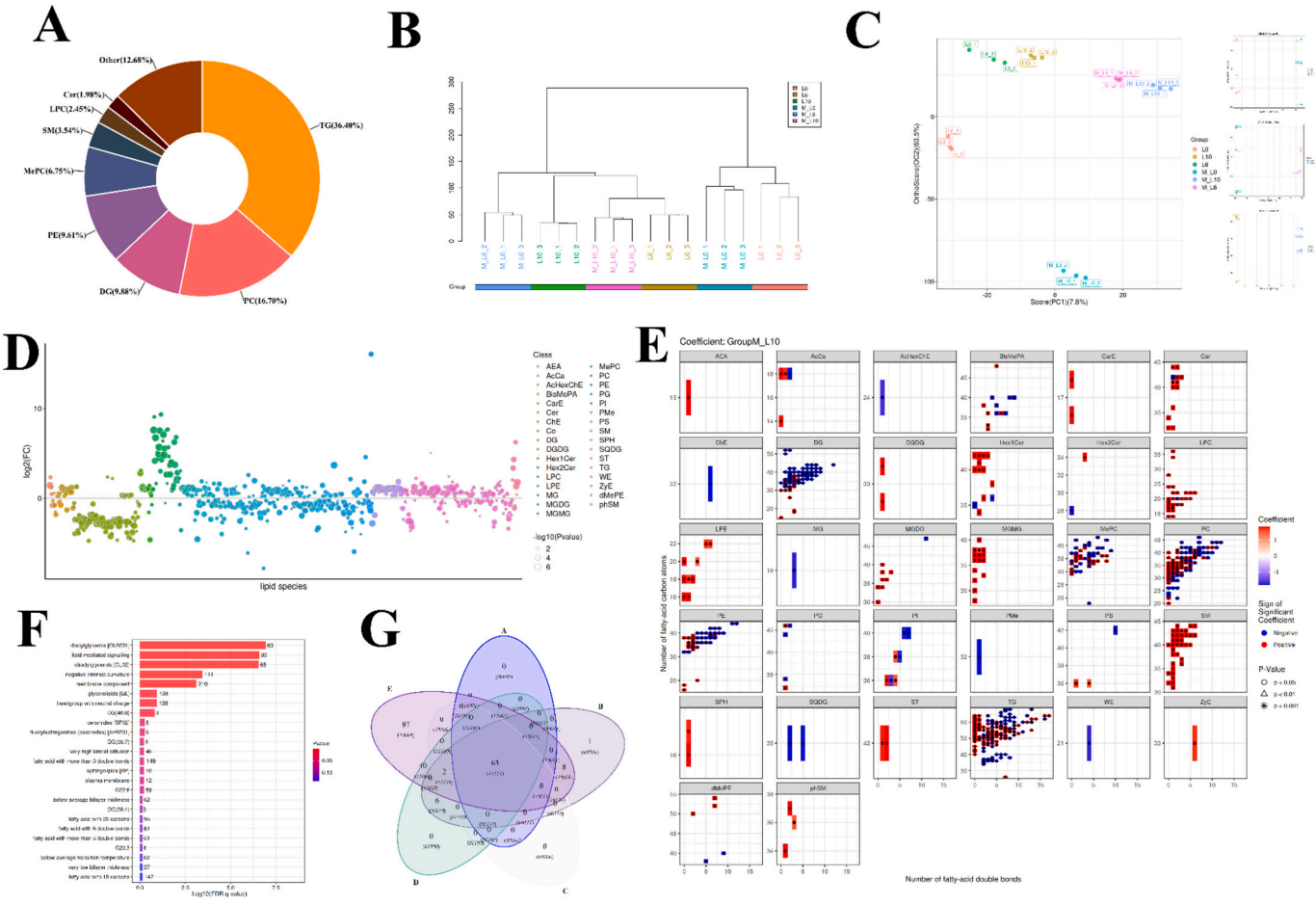

Fig. 3. The composition and classification of lipid species detected in lipid samples (L group and M/L group) identified by LC-MS-based lipidomics analysis (A); overall sample hierarchical clustering tree (B); OPLS-DA between groups (C); differential lipid bubble plot (D); heatmap of the structural characteristics of lipid differences (E); enrichment bar graph (F); the numerical labels on the bar graph indicate the number of differential lipids enriched to that item; Venn diagram of five LION pathways (G).

9.88 %), phosphatidylethanolamines (PEs, 141 species, 9.61 %), methylphosphatidylcholines (MePCs, 99 species, 6.75 %), sphingomyelins (SMs, 52 species, 3.54 %), lysophosphatidylcholines (LPCs, 36 species, 2.45 %), ceramides (Cers, 29 species, 1.98 %), and other lipids (186 species, 12.68 %) (Fig. 3A). According to Yan et al. (2022), TG, PC, and PE are the predominant lipid classes in fish tissues, consistent with the findings of this study. TGs play a crucial role as carriers of fatty acids and are the main form of energy storage in animal bodies. PCs and PEs are major components of phospholipids in aquatic muscle tissues, essential for regulating cell physical structure, membrane fluidity, and signal transduction. They also enhance microbial bioactivity and provide nutritional value (X.-Y. Wang et al., 2021). PC tends to induce fluidity within membranes, while PE contributes to membrane rigidity (Fang et al., 2022). Chen et al. reported that PC content is closely linked to the freshness of seafood (Chen et al., 2022), marking them as significant lipid metabolic products in seafood.

The overall differences in lipidomic profiles between sample solutions were interpreted using a hierarchical clustering tree (Fig. 3B). The results indicated significant differences between the two groups during storage. Additionally, an orthogonal partial least squares analysis (OPLS-DA) model was constructed to further elucidate these differences (Fig. 3C). The model's R^2X, R^2Y, and Q^2 values were 0.857, 0.988, and 0.7, respectively, indicating good predictive ability. The findings revealed significant differences between the two sample groups during cold storage, which is also evident in pairwise OPLS-DA comparisons. Overall, the distinct separation observed in the hierarchical clustering tree and OPLS-DA model between the L group and M/L group suggests that microbial growth significantly alters the lipid profile of grouper.

3.3.2. Differential lipid (DL) analysis

To further analyze the differences in lipid composition between the two groups of sample solutions during refrigeration, the detected 1467 lipids were screened using systematic analysis of calculated *P* values and OPLS-DA derived VIP thresholds. Five representative comparisons (within the same group, day 10 vs. day 0; at the same storage time, M/L vs. L) were statistically analyzed, with results shown in Table S1. Among these five comparisons, the least significant difference was observed in M/L0 vs. L0, likely because the microbial impact on grouper lipids in freshly prepared sample solutions was not yet evident. Within the same group, the most significant differences were observed in day 10 vs. day 0, identifying 920 (L group) and 854 (M/L group) differential lipids (DLs), indicating significant changes in the lipid profile of grouper with storage time. This finding aligns with the general trend of lipid changes in seafood during refrigeration. Additionally, in the comparisons of M/L6 vs. L6 and M/L10 vs. L10, the number of upregulated DLs significantly exceeded the downregulated ones, suggesting a pronounced impact of microbial activity on the evolution of grouper lipid profiles. For instance, in the M/L10 vs. L10 comparison, a bubble plot of differential lipids was generated (Fig. 3D), and the specific information on DLs is presented in Table S2. Among the 771 screened DLs, they were classified into 33 lipid categories, primarily including TG (176), PC (154), DG (108), PE (75), MePC (49), SM (43), and LPC (34).

TG is a neutral lipid, and according to Pongsetkul et al. (2017), neutral lipids exhibit a higher degree of lipolysis/oxidation. Consequently, TGs are more susceptible to oxidative stress, leading to the highest number of detected TGs, with 105 TGs being upregulated, accounting for 59.66 %. This indicates that microbial growth promotes lipid oxidation. PC and PE are major components of phospholipids in muscle tissues, maintaining normal cell membrane permeability. Polyunsaturated fatty acids like EPA and DHA mainly accumulate in PC and PE (H. Sun et al., 2020). Among the PCs and PEs, 95 were upregulated, comprising only 41.48 % of the total PC and PE lipids, suggesting that as nutrients (Sargent et al., 2003), PC and PE are utilized by microorganisms, leading to the downregulation of most PC and PE. DGs are natural components of edible lipids that can be hydrolyzed by lipases. The first step of oxidation is the conversion of triglycerides to oxidized triglyceride monomers, followed by the formation of triglyceride dimers and DGs. Additionally, glycerophospholipid breakdown also leads to DG accumulation (Wang, Wang, et al., 2020), indicating lipid oxidation in grouper lipids during refrigeration. Interestingly, out of 108 DGs, 94 were downregulated, accounting for 87.04 %, suggesting that accumulated DGs during refrigeration are utilized by microorganisms, promoting microbial growth. LPCs are intermediate metabolites of lecithin. LPCs have strong surface activity, causing cell membrane rupture and resulting in hemolysis or cell necrosis. Among the 34 screened LPCs, 33 were upregulated (97.06 %), with significant fold changes (FC), with 24 LPCs changing by more than tenfold, indicating a substantial microbial impact on LPCs, further promoting phospholipid oxidation and metabolism.

Additionally, the carbon number and saturation level (number of double bonds) of lipids were calculated to understand the diverse structural characteristics of lipids. Different DLs were categorized by their structure using a heatmap (Fig. 3E). DG, LPC, MePC, PC, PE, SM, and TG were identified as the primary DLs. Besides LPC and SM, which were almost entirely upregulated, the number of double bonds seemed to differentiate between upregulated and downregulated DLs: DLs with more than five double bonds were generally downregulated, while those with fewer than five double bonds were predominantly upregulated. This suggests that during microbial growth in the lipid solution, microorganisms mainly utilize polyunsaturated fatty acids, promoting lipid oxidation and generating fatty acids with fewer double bonds or saturated fatty acids.

In summary, the analysis of DLs indicated that microbial growth significantly impacted lipid profile changes. Certain DLs, such as PC, PE, and DG, accumulate and serve as substrates for microbial growth, particularly long-chain polyunsaturated fatty acids. Therefore, microbial growth and lipid oxidation/lipolysis interact synergistically, which is consistent with the findings in Sections 3.1 and 3.2.

3.3.3. Key differential lipids selection

To identify a set of key DLs that play crucial roles in the sample solutions, LION (Lipid Ontology) enrichment analysis was conducted, generating an enrichment bar chart (Fig. 4F). The top five LION pathways with more than 50 DLs are listed in Table S3, involving diacylglycerols [GL0201], lipid-mediated signaling, diradylglycerols [GL02], negative intrinsic curvature, and membrane components. Among the DLs related to these pathways, 63 different DLs were identified (Fig. 4G). Out of these, 44 DLs had VIP values greater than 1, including: DG (14:0_18:2); DG (15:0_18:1); DG (16:0_18:1); DG (16:0_18:2); DG (16:0_20:4); DG (16:0_20:5); DG (16:0_22:4); DG (16:0_22:5); DG (16:0_22:6); DG (16:1_18:2); DG (16:1_22:6); DG (17:1_18:2); DG (18:0_18:1); DG (18:0_18:2); DG (18:0_20:4); DG (18:0_22:4); DG (18:0_22:6); DG (18:1_14:0); DG (18:1_18:2); DG (18:1_20:2); DG (18:1_20:4); DG (18:1_20:5); DG (18:1_22:1); DG (18:1_22:2); DG (18:1_22:6); DG (18:2_18:2); DG (18:2_22:6); DG (18:3_18:2); DG (18:3_18:3); DG (18:4_16:0); DG (20:0_22:6); DG (20:1_18:1); DG (20:1_22:6); DG (20:2_18:2); DG (20:5_18:2); DG (22:0_22:6); DG (22:3_18:2); DG (22:6_22:6); DG (34:2); DG (36:3); DG (38:5); DG (42:9); DG (44:7); DG (52:2). These 44 DLs were ultimately selected as key DLs for further analysis regarding their relationship with microbial activity and the molecular mechanisms underlying the production of undesirable VOCs.

3.4. Microbiomics

3.4.1. Community richness and diversity

Illumina HiSeq sequencing generated a total of 503,820 raw 16S rRNA sequence reads of the V4 region from eighteen test sample sets. After quality control, approximately 335,807 high-quality bacterial tags were obtained. The alpha diversity and beta diversity indices of the microbial communities in the two sample solutions were analyzed to comprehensively evaluate their overall diversity. Alpha diversity

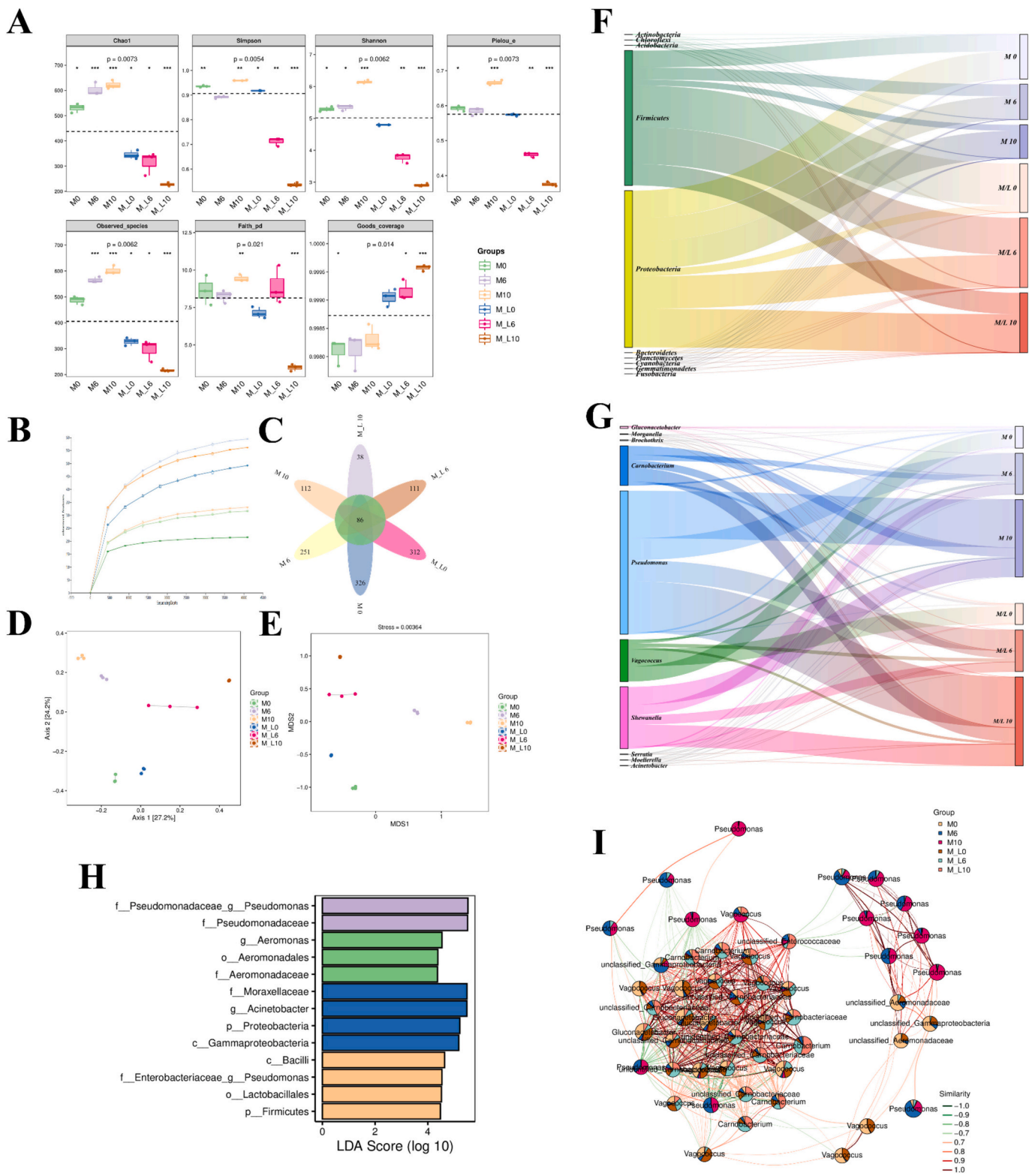

Fig. 4. Alpha diversity indices, including Chao1 and observed species (abundance), shannon diversity index, Faith's PD (phylogenetic diversity), and pielou's evenness, for M group and M/L group (A); dilution curve of gene sequence V4 region (B); Venn diagrams showing unique and shared OTUs of microbial communities (C); beta diversity analysis of two sample solutions based on PCoA (D) and NMDS (E); the richness of individual microbial species at the phylum (F) and genus (G) levels during cold storage; LEfSe analysis (H); and bacterial community network of different taxa (I).

reflects species richness, diversity, and evenness. In this study, Chao1 and Observed species indices represented richness, Shannon and Simpson indices represented diversity, Faith's PD index represented phylogenetic diversity, Pielou's evenness index represented evenness, and Good's coverage index represented coverage. Grouped box plots of alpha diversity are shown in Fig. 4A. The calculated Good's coverage values for microbial community richness ranged from 99.77 % to 99.96 %, indicating high coverage of the samples. The rarefaction curve of the

V4 region gene sequences (Fig. 4B) visually reflected the sampling depth, with all treatment groups showing a flattening trend, indicating that the sequencing results accurately reflected the microbial characteristics during the storage of the sample solutions.

The results of the diversity analysis were generally consistent (Fig. 4A), Specifically, OTUs exhibited a decreasing trend with storage time. Similar trends were observed in Chao1 and Faith's PD indices, indicating that storage time promotes the formation of dominant bacteria and reduces diversity. Additionally, it was found that within the same storage period, the OTUs in the M/L group showed a lower decline trend compared to the M group. This suggests that lipid oxidation also leads to reduced microbial diversity and promotes the formation of dominant bacteria. Based on OTU results, the petal diagram visualized the similarities and differences in microbial diversity among samples throughout the storage period (Fig. 4C). For samples stored at 4 °C, there were 86 core OTUs in the most overlapping region across all storage times. On day 0, there were 326 and 312 unique OTUs, respectively. After 10 days of storage, the number of unique OTUs decreased to 112 and 38, respectively, illustrating the reduction in microbial diversity during storage. Furthermore, PCoA and NMDS analyses were conducted to evaluate the beta diversity of the two groups of sample solutions. The results, as shown in Fig. 4(D-E), indicated that at the initial stage (day 0), the addition of grouper lipids to the bacterial solution did not significantly affect microbial diversity. However, significant differences emerged during storage, becoming more pronounced with extended storage time. This further indicates that lipid oxidation affects microbial diversity in the bacterial solution, and the changes in microbial diversity become more apparent as lipid oxidation progresses.

3.4.2. Changes in microbial diversity during storage of lipid sample solutions

To assess changes in microbial community structure, the abundance of individual microbial species at the phylum and genus levels was analyzed using 16S rRNA sequencing. The top 10 most abundant species are shown in Fig. 4(F-G).

At the phylum level (Fig. 4F), the main phyla detected in the refrigerated sample solutions were *Firmicutes* and *Proteobacteria*, accounting for over 95 % of all ASVs. Among these predominant phyla, the relative abundance of *Proteobacteria* increased with storage time, rising from 62.10 % on day 0 to 82.31 % on day 10. Conversely, the relative abundance of *Firmicutes* decreased from 37.89 % on day 0 to 17.69 % on day 10. Notably, the addition of lipid solutions enhanced these trends, suggesting that lipid oxidation may play a role in promoting shifts in microbial diversity.

At the genus level, Fig. 4G presents the top ten microbial genera. Among these, *Carnobacterium*, *Pseudomonas*, *Vagococcus*, *Shewanella*, and *Gluconacetobacter* were the dominant microbial groups in the sample solutions. With extended refrigeration time, the relative abundances of *Carnobacterium* (7.75 %–13.68 %), *Pseudomonas* (7.51 %–53.61 %), and *Shewanella* (5.30 %–24.90 %) gradually increased, while the relative abundance of *Vagococcus* decreased (69.54 %–6.65 %). Previous studies have identified that *Pseudomonas*, *Carnobacterium*, and *Shewanella* are major spoilage bacteria during the refrigeration of seafood (P. Li et al., 2022; Odeyemi et al., 2018; Shewan et al., 1960). Importantly, other microbial genera such as *Acinetobacter*, *Brochothrix*, *Moellerella*, *Morganella*, and *Serratia* were significantly inhibited after refrigeration, with relative abundances below 0.5 %. The reduction in the relative abundance of some microbial groups may be related to the production of antibacterial metabolites by dominant bacteria and their competitive disadvantage for available nutrients. (Marmion et al., 2021).

Combining these findings with the alpha diversity results, the enrichment of dominant microorganisms after refrigeration likely contributes to for the reduction in microbial diversity in the sample solutions. Additionally, Linear Discriminant Analysis Effect Size (LEfSe) analysis revealed that 13 biomarkers had LDA scores exceeding 4, indicating significant differences in microbial species between different groups, including *Actinobacteria*, *Pseudomonadaceae*, *Pseudomonas*, among others (Fig. 4H). The network of bacterial communities in different groups is shown in Fig. 4I. The bacterial community networks in both groups on day 6 had the lowest network density, suggesting higher crosstalk between resident bacteria. The clustering coefficient of the bacterial community networks in both groups on day 10 was the highest, indicating that the network tended to divide into subnetworks. The absence of network relationships between the newly prepared samples on day 0 and other groups suggests no correlation between the microbial communities of the fresh samples and the other samples.

3.5. VOCs

HS-SPME-GC–MS was employed to detect VOCs in the sample solutions during cold storage. A total of 48 VOCs were identified, including 1 acid, 13 alcohols, 7 aldehydes, 5 aromatic compounds, 8 hydrocarbons, 5 ketones, and 9 other types of compounds (4 nitrogen-containing compounds and 2 sulfur-containing compounds). These compounds were quantitatively analyzed using IS, as shown in Table 1. Nearly all VOCs exhibited a gradual increase during cold storage. Hydrocarbons were the main VOCs detected in the sample solutions during storage; however, hydrocarbons generally do not have strong odors, thus contributing little to the overall flavor.

Additionally, other types of VOCs showed varying degrees of increase, likely due to various biochemical reactions occurring in the sample solutions during storage (Zhao et al., 2022). These primarily included alcohols, aldehydes, ketones, and some nitrogen- and sulfur-containing compounds. The overall flavor was affected by these low-threshold compounds. To visualize the changing trends of different types of VOCs in the sample solutions during cold storage, the concentrations of the 48 VOCs were normalized, and a cluster heatmap was generated (Fig. 5A). In Fig. 5A, different types of VOCs are distinguished, with VOCs showing significant increases in concentration marked. Furthermore, OPLS-DA, which offers strong predictive power, was used to display differences between sample groups (Fig. 5B), and the variable importance in projection (VIP) values were generated and shown in Table 1.

Alcohols, aldehydes, ketones, and some nitrogen- and sulfur-containing compounds have low odor thresholds and can exhibit noticeable odors (Chu et al., 2024). Apart from hydrocarbons, alcohols showed the most significant changes, reaching 286.84 μg/L (M group), 492.32 μg/L (L group), and 654.65 μg/L (M/L group) by the end of storage. Alcohols are closely associated with characteristic fatty odors, primarily derived from the oxidation of polyunsaturated fatty acids and the reduction of methyl ketones (Cheng et al., 2023). Consequently, the alcohol content in the L group remained higher than that in the M group throughout storage, with the M/L group showing the highest alcohol content, likely due to the microbial promotion of lipid oxidation in the sample solutions. Notably, 1-octanol, 1-octen-3-ol, 2-nonanol, and 2-octanol exhibited the most significant changes. Due to their low odor thresholds, these compounds are considered major contributors to the overall flavor. According to a report by Li et al. (2020), 1-octen-3-ol, produced by the action of 12-lipoxygenase on arachidonic acid, is a highly representative VOC in seafood, providing fishy, fatty, mushroomy, and grassy flavors, consistent with the findings of this study.

Additionally, lipid oxidation leads to the formation of aldehydes and ketones (Zareian et al., 2018). Similar to alcohols, the presence of microorganisms promotes lipid oxidation, resulting in a 31.35 % and 25.43 % increase in the total content of aldehydes and ketones, respectively (M/L group vs. L group). These VOCs are associated with unpleasant, pungent, and spicy odors (Cheng et al., 2023; Sérot et al., 2001).

In addition to the primary VOCs detected, nitrogen- and sulfur-containing compounds also play a significant role in the overall odor of the sample solutions. According to VIP values, trimethylamine (1.45), methanethiol (1.11), and indolizine (1.51) are notable VOCs that

Table 1
VOCs content (μg/L sample solution) of grouper lipid solution during cold storage.

	Name	M group			L group			M/L group			
		M0	M6	M10	L0	L6	L10	M/L0	M/L6	M/L10	VIP
NO.	Acid										
1	Acetic acid	3.85 ± 0.22	7.3 ± 0.55	11.74 ± 0.9	ND	ND	5.99 ± 1.23	4.23 ± 0.36	9.5 ± 0.5	13.5 ± 0.96	0.34
Alcohol											
2	1-Dodecanol	ND	29.76 ± 0.35	74.48 ± 9.72	ND	34.89 ± 0.15	67.11 ± 13.71	ND	45.16 ± 1.32	91.11 ± 5.88	0.72
3	1-Hexanol	ND	ND	12.16 ± 0.32	ND	ND	21.66 ± 1.35	ND	17.65 ± 0.58	29.59 ± 2.18	1.24
4	1-Octanol	ND	ND	ND	ND	17.22 ± 0.77	20.89 ± 0.28	ND	15.91 ± 3.03	25.72 ± 1.52	1.43
5	1-Octen-3-ol	ND	ND	18.15 ± 1.8	4 ± 0.6	49.16 ± 3.97	71.01 ± 0.89	ND	84.51 ± 1.5	117.42 ± 2.11	1.41
6	1-Pentanol	ND	35.58 ± 3.66	74.55 ± 3.4	ND	40.97 ± 3.81	64.79 ± 0.53	ND	57.84 ± 3.53	86.41 ± 0.6	0.72
7	2-Hexadecanol	ND	ND	3.72 ± 3.72	ND	ND	5.53 ± 0.73	ND	ND	6.37 ± 0.78	0.59
8	2-Nonanol	ND	ND	25.71 ± 2	6.75 ± 1.09	31.52 ± 2.78	44.33 ± 0.17	7.83 ± 0.32	32.63 ± 0.97	51.12 ± 0.34	1.53
9	2-Octanol	ND	ND	10.92 ± 0.68	4.52 ± 1.26	12.1 ± 1.67	20.42 ± 0.04	5.17 ± 0.84	12.49 ± 1	23.49 ± 0.34	1.42
10	2-Tridecanol	ND	ND	10.23 ± 0.24	ND	ND	19.76 ± 1.2	ND	ND	22.8 ± 1.62	0.61
11	3-Methyl-1-butanol	ND	8.49 ± 1.26	23.37 ± 1.85	8.92 ± 1.18	28.89 ± 5.78	42.51 ± 0.45	9.26 ± 0.76	29.71 ± 4.26	51.91 ± 0.02	1.19
12	Heptanol	ND	ND	9.38 ± 0.27	ND	ND	12.77 ± 0.88	ND	ND	39.2 ± 2.87	0.67
13	Methyl alcohol	ND	ND	ND	493.53 ± 71.51	311.55 ± 40.08	80.5 ± 3.33	490.88 ± 10.45	281.28 ± 30.09	93.92 ± 5.15	1.91
14	Phenylethyl alcohol	7.92 ± 0.19	17.14 ± 1.38	24.15 ± 1.6	8.8 ± 1.4	20.6 ± 1.82	21.03 ± 2.54	ND	9.71 ± 0.52	15.57 ± 0.02	0.32
Aldehyde											
15	2,4-Decadienal	ND	ND	ND	ND	33.99 ± 2.02	63.26 ± 0.81	ND	38.73 ± 2.44	85.12 ± 5.76	1.6
16	2,4-Dimethyl-benzaldehyde	ND	ND	ND	ND	ND	10.46 ± 0.85	ND	8.9 ± 0.11	14.62 ± 1.85	1.43
17	2,4-Heptadienal	6.82 ± 0.37	11.88 ± 0.11	22.76 ± 2.72	ND	7.67 ± 0.52	14.78 ± 0.56	ND	7.54 ± 0.04	16.94 ± 0.86	0.13
18	2-Heptenal	ND	12.59 ± 0.07	40.71 ± 3.5	ND	17.89 ± 1.43	34.73 ± 0.5	ND	17.5 ± 0.59	39.55 ± 0.01	0.65
19	Benzaldehyde	21.2 ± 0.18	22.18 ± 1.55	29.66 ± 1.09	22.57 ± 2.23	37.93 ± 1.93	72.62 ± 2.39	25.08 ± 1.05	54.99 ± 2.08	112.49 ± 21.99	1.07
20	Hexanal	1.85 ± 0.09	ND	ND	2.1 ± 0.79	14.17 ± 0.61	24.64 ± 0.72	2.21 ± 0.59	17.08 ± 0.45	39.68 ± 8.35	1.37
21	Nonanal	6.01 ± 0.09	17.02 ± 1.55	48.13 ± 2.78	6.23 ± 0.47	26.61 ± 3.13	49.54 ± 0.84	6.92 ± 0.31	35.9 ± 0.15	84.96 ± 4.18	0.65
Aromatic compound											
22	1,2,4-Trimethyl-benzene	6.96 ± 0.01	11.65 ± 1.24	17.99 ± 1.19	ND	13.18 ± 0.57	18.16 ± 0.61	ND	16.12 ± 0.33	23.78 ± 1.4	0.06
23	1,3-Dimethyl-benzene	38.23 ± 1.72	53.75 ± 3.82	67.72 ± 2.6	50.96 ± 6.28	60.94 ± 4.23	58.59 ± 0.68	56.69 ± 1.71	74.9 ± 2.2	91.51 ± 1.79	0.5
24	1-Methyl-2-(1-methylethyl)-benzene	11.31 ± 1.21	24.3 ± 1.63	34.92 ± 0.23	25.7 ± 1.54	44.36 ± 4.6	56.82 ± 1.58	31.26 ± 5.83	54.71 ± 6.55	83.49 ± 2.12	0.84
25	Butylated hydroxytoluene	6.25 ± 0.51	12.82 ± 2.62	12.3 ± 0.92	6.67 ± 0.78	21.88 ± 0.88	16.27 ± 2.35	7.08 ± 0.03	18.61 ± 0.29	15.25 ± 1.46	0.39
26	2-methoxy-4-(1-propenyl)-phenol	ND	ND	8.5 ± 8.5	ND	10.24 ± 0.88	17.71 ± 2.06	ND	10.03 ± 0.25	24.2 ± 2.18	1.2
Hydrocarbon											
27	Azulene	ND	ND	ND	ND	ND	6.57 ± 1.49	1.06 ± 1.06	5.37 ± 0.02	8.61 ± 0.03	1.44
28	Decane	ND	58.21 ± 8.45	131.38 ± 3.1	ND	102.99 ± 5.54	173.75 ± 8.38	1.08 ± 1.08	93.02 ± 2.5	170.75 ± 4.48	0.87
29	Dodecane	ND	ND	148.97 ± 6.95	ND	157.62 ± 20.6	205.83 ± 4.7	25.28 ± 7.43	178.63 ± 3.73	188.41 ± 4.31	1.69
30	Heptadecane	20.58 ± 0.04	ND	32.86 ± 3.91	ND	229.96 ± 15.66	23.6 ± 0.76	2.21 ± 0.43	ND	33 ± 0.85	0.08
31	Hexadecane	ND	46.6 ± 22.83	90.88 ± 0.31	ND	116.72 ± 1.67	181.23 ± 9.65	36.24 ± 2.45	71.67 ± 3.67	180.33 ± 6.44	1.16

(*continued on next page*)

Table 1 (*continued*)

	Name	M group			L group			M/L group			
		M0	M6	M10	L0	L6	L10	M/L0	M/L6	M/L10	VIP
32	Octane	16.48 ± 1.55	33.12 ± 9.33	86.08 ± 0.78	ND	ND	74.28 ± 0.04	ND	ND	113.49 ± 5.65	0.53
33	Pentadecane	19.89 ± 2.96	ND	ND	ND	73.55 ± 8.19	85.36 ± 0.6	22.56 ± 3.67	56.46 ± 2.14	74.92 ± 5.43	1.29
34	Tetradecane	11.41 ± 0.16	52.62 ± 2.93	128.05 ± 0.2	13.39 ± 2.44	75.95 ± 4.83	92.36 ± 5.07	24.68 ± 0.81	73.04 ± 0.7	100.59 ± 11.83	0.52
Ketone											
35	2-Butanone	5.79 ± 0.06	12.17 ± 1.27	29.56 ± 0.06	ND	ND	10.45 ± 0.46	10.76 ± 0.74	15.12 ± 0.11	23.32 ± 0.87	0.35
36	2-Decanone	ND	ND	31.2 ± 1.52	ND	ND	16.91 ± 1.4	ND	ND	45.46 ± 2.52	0.59
37	2-Undecanone	20.81 ± 1.54	29.6 ± 1.24	48.42 ± 3.74	ND	11.89 ± 0.83	15.47 ± 1.25	23.15 ± 1.11	35.65 ± 0.81	59.61 ± 3.13	0.28
38	2-Octanone	ND	15.05 ± 0.37	27.04 ± 1.07	ND	12.61 ± 0.76	21.01 ± 0.9	ND	17.01 ± 0.21	22.25 ± 0.12	0.58
39	1-Phenyl-ethanone	ND	ND	ND	ND	7.04 ± 1.31	57.38 ± 46.96	2.85 ± 0.08	7.47 ± 0.81	11.91 ± 2.07	1.48
Other (Nitrogen-Containing)											
40	1H-Indole	12.27 ± 0.72	16.85 ± 0.96	27.92 ± 0.57	ND	ND	3.83 ± 1.67	13.36 ± 0.08	20.38 ± 0.04	25 ± 0.28	0.19
41	2-Methyl-quinoline	ND	1.9 ± 0.41	6.2 ± 0.01	ND	ND	ND	ND	11.94 ± 1.24	17.17 ± 0.67	0.73
42	Hydrazine	ND	108.4 ± 6.53	174.16 ± 15.4	ND	ND	ND	ND	132.81 ± 3.05	186.39 ± 0.58	0.5
43	Trimethylamine	ND	ND	161.48 ± 22.49	ND	ND	ND	ND	ND	246.99 ± 0.95	1.45
Other (Sulfur-Containing)											
44	Dimethyl sulfide	ND	96.57 ± 3.92	88.33 ± 70.46	ND	ND	ND	ND	108.48 ± 2.82	158.58 ± 5.92	0.64
45	Methanethiol	ND	107.4 ± 7.01	167.46 ± 2.26	ND	ND	ND	ND	135.09 ± 0.31	189.92 ± 8.55	1.11
Other											
46	2-Ethyl-furan	ND	ND	ND	13.69 ± 4.01	ND	60.95 ± 13.95	ND	28.63 ± 2.38	136.37 ± 0.3	1.59
47	Chloroform	ND	ND	ND	1143.56 ± 116.86	303.65 ± 71.39	57.44 ± 5.81	1200.81 ± 3.12	267.51 ± 4.33	65.37 ± 18.08	1.83
48	Indolizine	ND	29.95 ± 0.82	332.94 ± 0.65	ND	ND	ND	ND	36.01 ± 1.15	308.35 ± 11.73	1.51

All results are expressed as mean ± standard deviation. VIP is variable importance in projection (obtained through OPLS-DA).

accumulate over the storage period. Trimethylamine, a product of trimethylamine oxide reduction, imparts a putrid odor, while indolizine, derived from the catalytic action of tryptophanase, contributes a foul odor and stench. Both compounds are well-documented markers of fish spoilage (J. Huang et al., 2021; Leduc et al., 2012; Lou et al., 2023). Additionally, methanethiol, primarily produced through microbial activity and protein degradation, was also detected. Given that protein factors were controlled in this study, the methanethiol produced can be attributed to microbial action. Methanethiol was not detected in the L group, while its content increased by 11.83 % on the day 10 (M/L group vs. M group), indicating that lipid oxidation also accelerates microbial growth. These findings suggest that both microbial activity and lipid oxidation have an irreversible impact on the odor of fish. These processes are closely linked to the production of VOCs during the refrigerated storage of grouper.

3.6. Potential relationship between VOCs, lipid component evolution, and microbial growth

In previous analyses, the interaction between microbial growth and lipid degradation was established. To further visualize the relationship between the dominant microbial genera and DLs in the sample solutions during cold storage, a correlation heatmap was generated using the Mantel test (Fig. 5C). The results identified five significantly correlated microbial genera (*Carnobacterium*, *Pseudomonas*, *Gluconacetobacter*, *Vagococcus*, and *Shewanella*) and 30 DLs. *Pseudomonas*, *Gluconacetobacter*, and *Vagococcus* exhibited a strong correlation with almost all DLs (Mantel's $r \geq 0.4$, Mantel's $p < 0.01$), indicating their critical role in the production of DLs. For *Carnobacterium*, there were strong correlations with DG (18:0_18:1), DG (18:0_18:2), DG (18:2_18:2), and DG (44:7), with Mantel's r values ranging from 0.1 to 0.4, suggesting that these DLs are core to *Carnobacterium*. The heatmap also showed that these four DLs had no significant correlations with other DLs. Similarly, *Shewanella* showed significant correlations with DG (17:1_18:2), DG (18:0_22:4), and DG (20:0_22:6). Therefore, it can be inferred that the accumulation of DG (18:0_18:1), DG (18:0_18:2), DG (18:2_18:2), and DG (44:7) promotes the growth of *Carnobacterium*, while DG (17:1_18:2), DG (18:0_22:4), and DG (20:0_22:6) enhance the growth of *Shewanella*. Almost all DGs appear to stimulate the growth of *Pseudomonas* (e.g., DG (52:2)), *Gluconacetobacter* (e.g., DG (14:0_18:2), DG (16:0_18:2), DG (16:0_20:4), DG (16:0_20:5), DG (16:0_22:4), DG (16:1_18:2), DG (16:1_22:6), DG (18:1_14:0), DG (18:1_18:2), DG (18:1_20:5), DG (18:3_18:3), DG (18:4_16:0), DG (20:1_18:1), DG (20:1_22:6), DG (22:0_22:6), DG (22:6_22:6), DG (34:2), DG (36:3), DG (38:5), DG (42:9)), and *Vagococcus* (e.g., DG (15:0_18:1), DG (18:1_22:1)).

To further investigate the relationship between key microbial genera

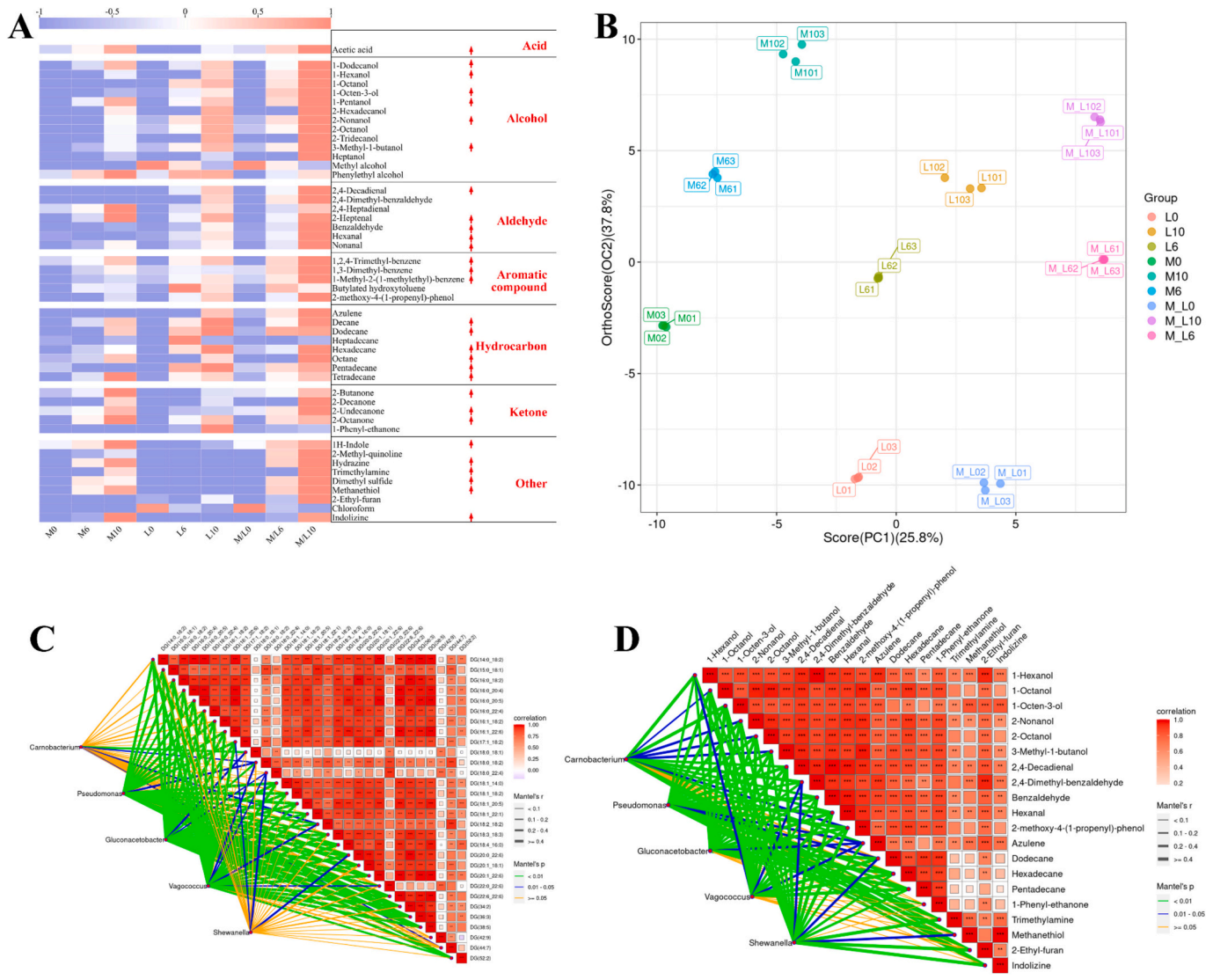

Fig. 5. The circular clustered heatmap of normalized VOCs (A) and OPLS-DA (B) for M group, L group, and M/L group. Mantel test of key microorganisms and differential lipids (C); mantel test of key microorganisms and Key VOCs.

and VOCs in the sample solutions during cold storage, a Mantel test was used to create a correlation heatmap (Fig. 5D). Similar to the previous analysis, *Carnobacterium*, *Pseudomonas*, *Gluconacetobacter*, *Vagococcus*, and *Shewanella* were identified as the most significantly correlated microbial genera. These can be considered the core VOC-producing microbes during the cold storage of the sample solutions. *Pseudomonas* and *Shewanella* showed significant correlations with nearly all key VOCs, likely because these two bacteria are the main microorganisms involved in the spoilage and deterioration of the grouper. Among the 20 VOCs with VIP values greater than 1, alcohols and ketones were most closely related to *Gluconacetobacter*, nitrogen- and sulfur-containing compounds were most closely related to *Shewanella*, and aldehydes were most closely related to both *Gluconacetobacter* and *Pseudomonas*. Combining this with the analysis of Fig. 5C, it is evident that these microorganisms utilize DLs during their growth process and produce detrimental VOCs. Specifically, DG (17:1_18:2), DG (18:0_22:4), and DG (20:0_22:6) may be closely related to nitrogen/sulfur-containing compounds, while DG (14:0_18:2), DG (52:2), and 21 other DGs might be associated with the production of alcohols, ketones, and aldehydes.

4. Conclusion

In this study, protein factors were excluded to investigate the interaction between lipids and microorganisms in refrigerated grouper and their impact on VOCs production. By evaluating the lipid characteristics (POV and TBARS) and microbial characteristics (biofilm mass and ATP content) in the lipid solution, it was determined that microbial growth promotes lipid oxidation, and the oxidation of grouper lipids similarly promotes microbial growth. Furthermore, lipidomics analysis was used to monitor the lipid composition of the lipid solution, identifying 44 differential lipids. Combined with microbial community diversity analysis, five key microorganisms (*Carnobacterium*, *Pseudomonas*, *Gluconacetobacter*, *Vagococcus*, and *Shewanella*) were identified. Using GC–MS, 20 key VOCs related to the odor changes in the grouper lipid solution were screened, establishing these five microorganisms as core odor producers. The study also identified the potential microbial and lipid sources of various VOCs categories (alcohols, aldehydes, ketones, nitrogen- and sulfur-containing compounds). This research reveals the potential interactions between lipids and microorganisms in flavor formation, providing new insights for improving seafood quality control.

Funding

This work was supported by the National Key Research and Development Program of China (2023YFD2401402), the earmarked fund for CARS-47, and the Shanghai Professional Technology Service Platform on Cold Chain Equipment Performance and Energy Saving Evaluation (19DZ2284000). All authors have read and agreed to the published version of the manuscript.

Institutional review board statement

In the present study, all procedures were performed in accordance with the "Guidelines for Experimental Animals" of the Ministry of Science and Technology (Beijing, China), and were approved by the Institutional Animal Care and Use Committee of Shanghai Ocean University (SHOU-DW-2023-087).

CRediT authorship contribution statement

Yuanming Chu: Writing – review & editing, Writing – original draft, Methodology, Investigation, Formal analysis, Data curation, Conceptualization. **Jinfeng Wang:** Writing – review & editing, Validation, Methodology, Funding acquisition. **Jing Xie:** Writing – review & editing, Supervision, Funding acquisition, Conceptualization.

Declaration of competing interest

The authors declare that they have no known competing financial interests or personal relationships that could have appeared to influence the work reported in this paper.

Appendix A. Supplementary data

Supplementary data to this article can be found online at https://doi.org/10.1016/j.fochx.2025.102183.

Data availability

Raw data for lipidomic analysis are available at: https://www.biodeep.cn/

References

Abd El-Hack, M. E., El-Saadony, M. T., Elbestawy, A. R., Ellakany, H. F., Abaza, S. S., Geneedy, A. M., … El-Tarabily, K. A. (2022). Undesirable odour substances (geosmin and 2-methylisoborneol) in water environment: Sources, impacts and removal strategies. *Marine Pollution Bulletin, 178*, Article 113579. https://doi.org/10.1016/j.marpolbul.2022.113579

Aiassa, V., Barnes, A. I., & Albesa, I. (2014). Macromolecular oxidation in planktonic population and biofilms of Proteus mirabilis exposed to ciprofloxacin. *Cell Biochemistry and Biophysics, 68*(1), 49–54. https://doi.org/10.1007/s12013-013-9693-6

Aracati, M. F., Rodrigues, L. F., de Oliveira, S. L., Rodrigues, R. A., Conde, G., Cavalcanti, E. N. F., … de Andrade Belo, M. A. (2022). Astaxanthin improves the shelf-life of tilapia fillets stored under refrigeration. *Journal of the Science of Food and Agriculture, 102*(10), 4287–4295. https://doi.org/10.1002/jsfa.11780

Chen, J., Kong, Q., Sun, Z., & Liu, J. (2022). Freshness analysis based on lipidomics for farmed Atlantic salmon (Salmo salar L.) stored at different times. *Food Chemistry, 373*, Article 131564. https://doi.org/10.1016/j.foodchem.2021.131564

Cheng, H., Wang, J., & Xie, J. (2023). Progress on odor deterioration of aquatic products: Characteristic volatile compounds, analysis methods, and formation mechanisms. *Food Bioscience, 53*, Article 102666. https://doi.org/10.1016/j.fbio.2023.102666

Chu, Y., Mei, J., & Xie, J. (2023a). Integrated volatile compounds and non-targeted metabolomics analysis reveal the characteristic flavor formation of proteins in grouper (Epinephelus coioides) during cold storage. *Food Research International, 172*, Article 113145. https://doi.org/10.1016/j.foodres.2023.113145

Chu, Y., Mei, J., & Xie, J. (2023b). Exploring the effects of lipid oxidation and free fatty acids on the development of volatile compounds in grouper during cold storage based on multivariate analysis. *Food Chemistry: X, 20*, Article 100968. https://doi.org/10.1016/j.fochx.2023.100968

Chu, Y., Wang, J., & Xie, J. (2024). Exploring the correlation of microbial community diversity and succession with protein degradation and impact on the production of volatile compounds during cold storage of grouper (Epinephelus coioides). *Food Chemistry, 460*, Article 140469. https://doi.org/10.1016/j.foodchem.2024.140469

Deng, W., Hamilton-Kemp, T. R., Nielsen, M. T., Andersen, R. A., Collins, G. B., & Hildebrand, D. F. (1993). Effects of six-carbon aldehydes and alcohols on bacterial proliferation. *Journal of Agricultural and Food Chemistry, 41*(3), 506–510. https://doi.org/10.1021/jf00027a030

Deng, Y., Wang, R., Wang, Y., Sun, L., Tao, S., Li, X., Gooneratne, R., & Zhao, J. (2020). Diversity and succession of microbial communities and chemical analysis in dried Lutianus erythropterus during storage. *International Journal of Food Microbiology, 314*, Article 108416. https://doi.org/10.1016/j.ijfoodmicro.2019.108416

Fang, C., Chen, H., Yan, H., Shui, S., Benjakul, S., & Zhang, B. (2022). Investigation of the changes in the lipid profiles in hairtail (Trichiurus haumela) muscle during frozen storage using chemical and LC/MS-based lipidomics analysis. *Food Chemistry, 390*, Article 133140. https://doi.org/10.1016/j.foodchem.2022.133140

Huang, J., Zhou, Y., Chen, M., Huang, J., Li, Y., & Hu, Y. (2021). Evaluation of negative behaviors for single specific spoilage microorganism on little yellow croaker under modified atmosphere packaging: Biochemical properties characterization and spoilage-related volatiles identification. *LWT, 140*, Article 110741. https://doi.org/10.1016/j.lwt.2020.110741

Huang, X., Tu, Z., Liu, W., Wu, C., & Wang, H. (2023). Effect of three culture patterns on quality changes of crayfish meats during partial freezing storage. *Food Chemistry, 414*, Article 135683. https://doi.org/10.1016/j.foodchem.2023.135683

Leduc, F., Krzewinski, F., Le Fur, B., N'Guessan, A., Malle, P., Kol, O., & Duflos, G. (2012). Differentiation of fresh and frozen/thawed fish, European sea bass (Dicentrarchus labrax), gilthead seabream (Sparus aurata), cod (Gadus morhua) and salmon (Salmo salar), using volatile compounds by SPME/GC/MS. *Journal of the Science of Food and Agriculture, 92*(12), 2560–2568. https://doi.org/10.1002/jsfa.5673

Li, P., Chen, Z., Tan, M., Mei, J., & Xie, J. (2020). Evaluation of weakly acidic electrolyzed water and modified atmosphere packaging on the shelf life and quality of farmed puffer fish (<scp> *Takifugu obscurus* </scp>) during cold storage. *Journal of Food Safety, 40*(3). https://doi.org/10.1111/jfs.12773

Li, P., Mei, J., Tan, M., & Xie, J. (2022). Effect of CO2 on the spoilage potential of Shewanella putrefaciens target to flavour compounds. *Food Chemistry, 397*, Article 133748. https://doi.org/10.1016/j.foodchem.2022.133748

Li, Q., Zhao, Y., Zhu, D., Pang, X., Liu, Y., Frew, R., & Chen, G. (2017). Lipidomics profiling of goat milk, soymilk and bovine milk by UPLC-Q-Exactive Orbitrap mass spectrometry. *Food Chemistry, 224*, 302–309. https://doi.org/10.1016/j.foodchem.2016.12.083

Liu, L., Zhao, Y., Zeng, M., & Xu, X. (2024). Research progress of fishy odor in aquatic products: From substance identification, formation mechanism, to elimination pathway. *Food Research International, 178*, Article 113914. https://doi.org/10.1016/j.foodres.2023.113914

Lou, X., Wen, X., Chen, L., Shu, W., Wang, Y., Hoang, T. T., & Yang, H. (2023). Changes in texture, rheology and volatile compounds of golden pomfret sticks inoculated with Shewanella baltica during spoilage. *Food Chemistry, 404*, Article 134616. https://doi.org/10.1016/j.foodchem.2022.134616

Marmion, M., Ferone, M. T., Whyte, P., & Scannell, A. G. M. (2021). The changing microbiome of poultry meat; from farm to fridge. *Food Microbiology, 99*, Article 103823. https://doi.org/10.1016/j.fm.2021.103823

Mukherjee, M., Zaiden, N., Teng, A., Hu, Y., & Cao, B. (2020). Shewanella biofilm development and engineering for environmental and bioenergy applications. *Current Opinion in Chemical Biology, 59*, 84–92. https://doi.org/10.1016/j.cbpa.2020.05.004

Odeyemi, O. A., Burke, C. M., Bolch, C. C. J., & Stanley, R. (2018). Seafood spoilage microbiota and associated volatile organic compounds at different storage temperatures and packaging conditions. *International Journal of Food Microbiology, 280*, 87–99. https://doi.org/10.1016/j.ijfoodmicro.2017.12.029

Pongsetkul, J., Benjakul, S., Vongkamjan, K., Sumpavapol, P., & Osako, K. (2017). Changes in lipids of shrimp (Acetes vulgaris) during salting and fermentation. *European Journal of Lipid Science and Technology, 119*(11). https://doi.org/10.1002/ejlt.201700253

Santos, C., Roseiro, C., Gonçalves, H., Aleixo, C., Moniz, C., & da Ponte, D. J. B. (2019). Susceptibility of dry-cured tuna to oxidation and biogenic amines generation related to microbial status and salting/curing technology. *LWT, 115*, Article 108420. https://doi.org/10.1016/j.lwt.2019.108420

Sargent, J. R., Tocher, D. R., & Bell, J. G. (2003). The lipids. In *Fish nutrition* (pp. 181–257). Elsevier. https://doi.org/10.1016/B978-012319652-1/50005-7.

Sérot, T., Regost, C., Prost, C., Robin, J., & Arzel, J. (2001). Effect of dietary lipid sources on odour-active compounds in muscle of turbot (Psetta maxima). *Journal of the Science of Food and Agriculture, 81*(14), 1339–1346. https://doi.org/10.1002/jsfa.950

Shewan, J. M., Hobbs, G., & Hodgkiss, W. (1960). The pseudomonas and achromobacter groups of bacteria in the spoilage of marine white fish. *Journal of Applied Bacteriology, 23*(3), 463–468. https://doi.org/10.1111/j.1365-2672.1960.tb00217.x

Shui, S., Yan, H., Tu, C., Benjakul, S., Aubourg, S. P., & Zhang, B. (2022). Cold-induced denaturation of muscle proteins in hairtail (Trichiurus lepturus) during storage: Physicochemical and label-free based proteomics analyses. *Food Chemistry: X, 16*, Article 100479. https://doi.org/10.1016/j.fochx.2022.100479

Silveira Alexandre, A. C., Corrêa Albergaria, F., dos Santos Ferraz Esilva, L. M., Carneiro Fernandes, L. A., de Sousa Gomes, M. E., & Pimenta, C. J. (2022). Effect of natural and synthetic antioxidants on oxidation and storage stability of mechanically separated tilapia meat. *LWT, 154*, Article 112679. https://doi.org/10.1016/j.lwt.2021.112679

Soler-Arango, J., Figoli, C., Muraca, G., Bosch, A., & Brelles-Mariño, G. (2019). The Pseudomonas aeruginosa biofilm matrix and cells are drastically impacted by gas discharge plasma treatment: A comprehensive model explaining plasma-mediated

biofilm eradication. *PLoS One, 14*(6), Article e0216817. https://doi.org/10.1371/journal.pone.0216817

Sun, H., Song, Y., Zhang, H., Zhang, X., Liu, Y., Wang, X., … Xue, C. (2020). Characterization of lipid composition in the muscle tissue of four shrimp species commonly consumed in China by UPLC−triple TOF−MS/MS. *LWT, 128*, Article 109469. https://doi.org/10.1016/j.lwt.2020.109469

Sun, Y., Hua, Q., Tian, X., Xu, Y., Gao, P., & Xia, W. (2022). Effect of starter cultures and spices on physicochemical properties and microbial communities of fermented fish (Suanyu) after fermentation and storage. *Food Research International, 159*, Article 111631. https://doi.org/10.1016/j.foodres.2022.111631

Tian, L., Wang, X., Liu, R., Zhang, D., Wang, X., Sun, R., Guo, W., Yang, S., Li, H., & Gong, G. (2021). Antibacterial mechanism of thymol against Enterobacter sakazakii. *Food Control, 123*, Article 107716. https://doi.org/10.1016/j.foodcont.2020.107716

Tu, C., Qi, X., Shui, S., Lin, H., Benjakul, S., & Zhang, B. (2022). Investigation of the changes in lipid profiles induced by hydroxyl radicals in whiteleg shrimp (Litopenaeus vannamei) muscle using LC/MS-based lipidomics analysis. *Food Chemistry, 369*, Article 130925. https://doi.org/10.1016/j.foodchem.2021.130925

Wang, J., Wang, Q., Xu, L., & Sun, D.-W. (2022). Effects of extremely low frequency pulsed electric field (ELF-PEF) on the quality and microstructure of tilapia during cold storage. *LWT, 169*, Article 113937. https://doi.org/10.1016/j.lwt.2022.113937

Wang, L., Wang, L., Qiu, J., & Li, Z. (2020). Effects of superheated steam processing on common buckwheat grains: Lipase inactivation and its association with lipidomics profile during storage. *Journal of Cereal Science, 95*, Article 103057. https://doi.org/10.1016/j.jcs.2020.103057

Wang, X.-Y., Xie, J., & Chen, X.-J. (2021). Differences in lipid composition of bigeye tuna (Thunnus obesus) during storage at 0 °C and 4 °C. *Food Research International, 143*, Article 110233. https://doi.org/10.1016/j.foodres.2021.110233

Wu, M., Tian, L., Fu, J., Liao, S., Li, H., Gai, Z., & Gong, G. (2022). Antibacterial mechanism of Protocatechuic acid against Yersinia enterocolitica and its application in pork. *Food Control, 133*, Article 108573. https://doi.org/10.1016/j.foodcont.2021.108573

Xue, C., You, J., Zhang, H., Zhao, L., Xiong, S., Yin, T., & Huang, Q. (2022). Hydrophobic bonds-dominated key off-odors/silver carp myofibrillar protein interactions, and their binding characteristics at cold storage and oral temperatures. *Food Chemistry: X, 15*, Article 100396. https://doi.org/10.1016/j.fochx.2022.100396

Yan, H., Jiao, L., Fang, C., Benjakul, S., & Zhang, B. (2022). Chemical and LC–MS-based lipidomics analyses revealed changes in lipid profiles in hairtail (Trichiurus haumela) muscle during chilled storage. *Food Research International, 159*, Article 111600. https://doi.org/10.1016/j.foodres.2022.111600

Yang, Z., Chu, Y., Zhang, C., Yan, J., & Xie, J. (2023). Changes in the physicochemical properties of grouper (Epinephelus coioides) fillets stored under vacuum packaging at chilly temperature contributing with the spoilage bacteria. *Food Bioscience, 55*, Article 103017. https://doi.org/10.1016/j.fbio.2023.103017

Yu, D., Xu, Y., Regenstein, J. M., Xia, W., Yang, F., Jiang, Q., & Wang, B. (2018). The effects of edible chitosan-based coatings on flavor quality of raw grass carp (Ctenopharyngodon idellus) fillets during refrigerated storage. *Food Chemistry, 242*, 412–420. https://doi.org/10.1016/j.foodchem.2017.09.037

Zareian, M., Böhner, N., Loos, H. M., Silcock, P., Bremer, P., & Beauchamp, J. (2018). Evaluation of volatile organic compound release in modified atmosphere-packaged minced raw pork in relation to shelf-life. *Food Packaging and Shelf Life, 18*, 51–61. https://doi.org/10.1016/j.fpsl.2018.08.001

Zhang, Q., Chen, X., Ding, Y., Ke, Z., Zhou, X., & Zhang, J. (2021). Diversity and succession of the microbial community and its correlation with lipid oxidation in dry-cured black carp (Mylopharyngodon piceus) during storage. *Food Microbiology, 98*, Article 103686. https://doi.org/10.1016/j.fm.2020.103686

Zhao, D., Hu, J., & Chen, W. (2022). Analysis of the relationship between microorganisms and flavour development in dry-cured grass carp by high-throughput sequencing, volatile flavour analysis and metabolomics. *Food Chemistry, 368*, Article 130889. https://doi.org/10.1016/j.foodchem.2021.130889

Zhou, X., Zhou, D.-Y., Liu, Z.-Y., Yin, F.-W., Liu, Z.-Q., Li, D.-Y., & Shahidi, F. (2019). Hydrolysis and oxidation of lipids in mussel Mytilus edulis during cold storage. *Food Chemistry, 272*, 109–116. https://doi.org/10.1016/j.foodchem.2018.08.019

Zhuang, S., Tan, Y., Hong, H., Li, D., Zhang, L., & Luo, Y. (2022). Exploration of the roles of spoilage bacteria in degrading grass carp proteins during chilled storage: A combined metagenomic and metabolomic approach. *Food Research International, 152*, Article 110926. https://doi.org/10.1016/j.foodres.2021.110926